Tumor growth delay by adjuvant alternating electric fields which appears non-thermally mediated

Quim Castellví [a,*], Mireia M. Ginestà [b], Gabriel Capellà [b], Antoni Ivorra [a]

[a] Universitat Pompeu Fabra, Barcelona, Spain
[b] Institut Català d'Oncologia-IDIBELL, Hospital Duran i Reynals, l'Hospitalet de Llobregat, Spain

ARTICLE INFO

ABSTRACT

Delivery of the so-called Tumor Treatment Fields (TTFields) has been proposed as a cancer therapy. These are low magnitude alternating electric fields at frequencies from 100 to 300 kHz which are applied continuously in a non-invasive manner. Electric field delivery may produce an increase in temperature which cannot be neglected. We hypothesized that the reported results obtained by applying TTFields in vivo could be due to heat rather than to electrical forces as previously suggested. Here, an in vivo study is presented in which pancreatic tumors subcutaneously implanted in nude mice were treated for a week either with mild hyperthermia (41 °C) or with TTFields (6 V/cm, 150 kHz) and tumor growth was assessed. Although the TTFields applied singly did not produce any significant effect, the combination with chemotherapy did show a delay in tumor growth in comparison to animals treated only with chemotherapy (median relative reduction = 47%). We conclude that concomitant chemotherapy and TTFields delivery show a beneficial impact on pancreatic tumor growth. Contrary to our hypothesis, this impact is non-related with the induced temperature increase.

© 2015 Elsevier B.V. All rights reserved.

1. Introduction

Delivery of the so-called Tumor Treatment Fields (TTFields) has been proposed as a novel local cancer therapy [1]. It is considered as a non-invasive method. Multiple surface electrodes distributed around the region where the tumor is located are connected to a device responsible for applying mild sinusoidal alternating electrical currents for the treatment. According to the researchers that have promoted the use of TTFields, applying these electric fields to living cells causes misalignment of internal molecules during cell division. This results in an inability to complete the mitotic process, and consequently, an anti-proliferative effect [2]. In contrast to normal mitosis which takes less than 1 h, during in vitro experiments it was reported that cells under electric fields tried to split during hours. Some cells go directly into apoptotic death and other end up dividing wrongly and finally die [1,3].

In vivo studies show a lower tumor growth rate for treated tumors compared to control ones [1,4,5]. Additionally, increase in treatment efficacy when TTFields are combined with conventional chemotherapy drugs is also reported [6,7].

The first human trial was performed in patients with glioblastomas (GBM). This type of brain tumor is associated with one of the worst cancer prognoses. The first results showed that the median overall survival of treated patients doubled the reported medians of historical control

patients [5]. However in a recent phase III clinical trial, the effect in GBM from patients treated with TTFields against the outcomes from patients treated with standard chemotherapy was reassessed [8]. In this study, no benefit was observed with TTFields in comparison to chemotherapy, despite the fact that chemotherapy has a very low effectiveness in the treatment of GBM [9,10]. Nevertheless, researchers that promote TTFields point to the fact that patients get a better quality of life for the same treatment outcome.

During in vitro assays TTFields were found to achieve maximum efficacy with frequencies between 100 kHz and 300 kHz [3,5]. The magnitude of the signal is adjusted so that an electric field magnitude typically in the range from 1 V/cm to 3 V/cm is obtained in the tumor [2]. For cancer treatment it has been established that this electric field has to be almost permanently applied and portable systems have been developed for such purpose [4]. In 2011 a device developed by the TTFields promoters obtained the approval of the U.S. Food and Drug Administration (FDA).

TTFields promoters claim that the employed electric field magnitudes are incapable of producing a significant increase in temperature [4]. However, it is possible to numerically demonstrate that TTFields delivery to living tissues must surely produce temperature increases of at least a few tenths of degree Celsius. As an illustration, we have performed a simulation of an experimental in vivo setup employed by TTFields promoters which shows that tissue temperature increases an average of 1.5 °C (simulation description and results are available on appendix). Most likely these are transient harmless temperature increases which are, for the most part, compensated by the organism

* Corresponding author at: Universitat Pompeu Fabra, 138 Roc Boronat, Barcelona, Spain.
E-mail address: quim.castellvi@upf.edu (Q. Castellví).

thermoregulatory mechanisms (e.g. vasodilation). If that is the case, then it can be supposed that these thermoregulatory responses may have a non-negligible effect on tumor growth, particularly if TTFields delivery is accompanied by chemotherapy. Therefore, in our opinion, due to its magnitude and duration, heat injection by TTFields delivery either causes a local temperature increase or it triggers thermoregulatory responses which cannot be considered as negligible if the action mechanism of TTFields has to be elucidated.

The use of alternating electric fields for heating living tissues is a common therapeutic technique. In the context of cancer treatments, hyperthermia is used as an adjuvant to a primary treatment such as chemotherapy or radiotherapy [11,12]. In these cases, it has been hypothesized that the beneficial impact of hyperthermia is both direct (i.e. thermally mediated) and indirect through physiological responses, such as vasodilation, to the temperature increase [13]. Hyperthermia therapies are commonly applied in short sessions, about an hour, inducing tissue temperatures from 40 to 44 °C [13]. Although it has been shown that cell survival at slightly elevated temperatures not only depends on the temperature but also on the exposure time [14], to the best of our knowledge, it has not been tested in vivo whether a prolonged exposure to mild temperatures could be beneficial for the treatment of cancer.

Since TTFields treatments produce a significant increase in temperature (or trigger significant thermoregulatory responses) and these are present continuously for weeks, we hypothesized that the positive results of these treatments are not due to the direct effect of the electric fields on the mitotic process but to an effect mediated by the prolonged mild hyperthermia that the delivery of those fields causes. To test this hypothesis we induced 1-week mild hyperthermia on a subcutaneously implanted patient derived xenograft in mice by means of a heat applicator which did not deliver electric fields to tissues. In addition, since there are no independent in vivo studies that validate the efficacy of TTFields delivery in tumor proliferation, we also performed 1-week TTFields delivery in the same tumor model. Both treatments were applied singly and in combination with gemcitabine to reveal any possible synergetic effect.

2. Materials and methods

2.1. Treatment devices

Due to animal welfare criteria, animal immobilization for treatment was ruled out and a system based on the use of wearable treatment capsules was conceived (Scheme 1).

Two types of capsules were implemented; one for each treatment modality (Scheme 2). Actuators and sensors were contained within the capsules for applying the treatments. The capsules were built from polymethyl methacrylate (PMMA) and the actuators were fixed inside using epoxy resin (Fig. 1A–B). To apply the thermal treatment, a 0.5 W power resistor of 240 Ω was used as a heater element. In this capsule a PTC thermistor, used as thermal sensor, was attached on a thin latex strip and placed on the bottom part allowing the control the skin temperature. In addition an open silicon tube allowed air renewal thus reducing humidity for proper skin transpiration. In the capsule for TTFields delivery, stainless steel parallel plates were used to produce a uniform electric field between them. For improving the uniformity of the electric field, and as reported in previous studies [15,16], a mild conductivity gel (Aquasonic 100, Parker Laboratories, Inc., Fairfield, NJ, USA), with 0.2 S/m [15], was introduced in the 4 mm gap between plates before applying the capsule to the animal. During treatment, this gel was replaced approximately every 2 days to compensate for possible losses due to evaporation.

The capsules were attached to the mice using silicone harnesses (CiH62, Instech Laboratories, Inc., Plymouth Meeting, PA, USA) customized with thicker silicone tubes around the straps for increasing the skin contact and thus minimizing irritation (Fig. 1C).
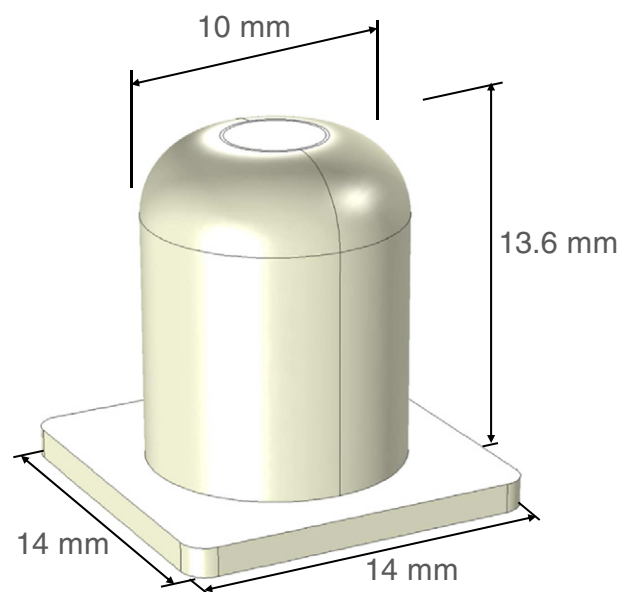
**Scheme 1.** Representation of the wearable capsules used during the study.

Electronic units capable of generating the signals for applying the treatments continuously were designed and developed. The hyperthermia electronic units, able to warm tissues in the capsule up to 43 °C, basically consist in a feedback control system where the skin temperature is measured with the thermistor inside the capsule. The electric field units consist of a square wave generator followed by low pass filter which produces a sinusoidal alternate voltage at 150 kHz.

The electrical connections between the electronic units and the capsules consist of thin insulated wires within a metal spring acting as a protection shield. A counterweight system (CM375BP, Instech Laboratories, Inc., Plymouth Meeting, PA, USA), mounted on the top of the animal's cage, ensures free mobility while preventing wire entanglement (Fig. 2A). A total amount of ten systems were built, five for each treatment type (Fig. 2B).

2.1.1. Treatment simulation

The geometry of the capsules was designed and evaluated with the aid of electrical and thermal numerical simulations. The Finite Element Method (FEM) was employed similarly to previously reported studies [17–20]. Specific FEM simulation software (COMSOL Multiphysics, v.4.3, COMSOL AB, Stockholm, Sweden) was used to solve the differential equations related to electrical and thermal physics.

Tissue temperature (T) at time (t) due to applied heat (Q) was obtained using the *Pennes Bioheat Equation* Eq. (1) [21]. For each tissue with defined density (ρ), heat capacity (c), thermal conductivity (k) and blood perfusion (ω_b), the heat dissipated by blood circulation depends on the density (ρ_b) and heat capacity (c_b) of the blood and also
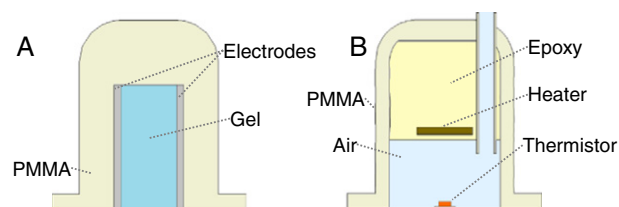
Scheme 2. (A) Sketch of capsule to apply alternating electric fields. (B) Sketch of capsule to apply hyperthermia.
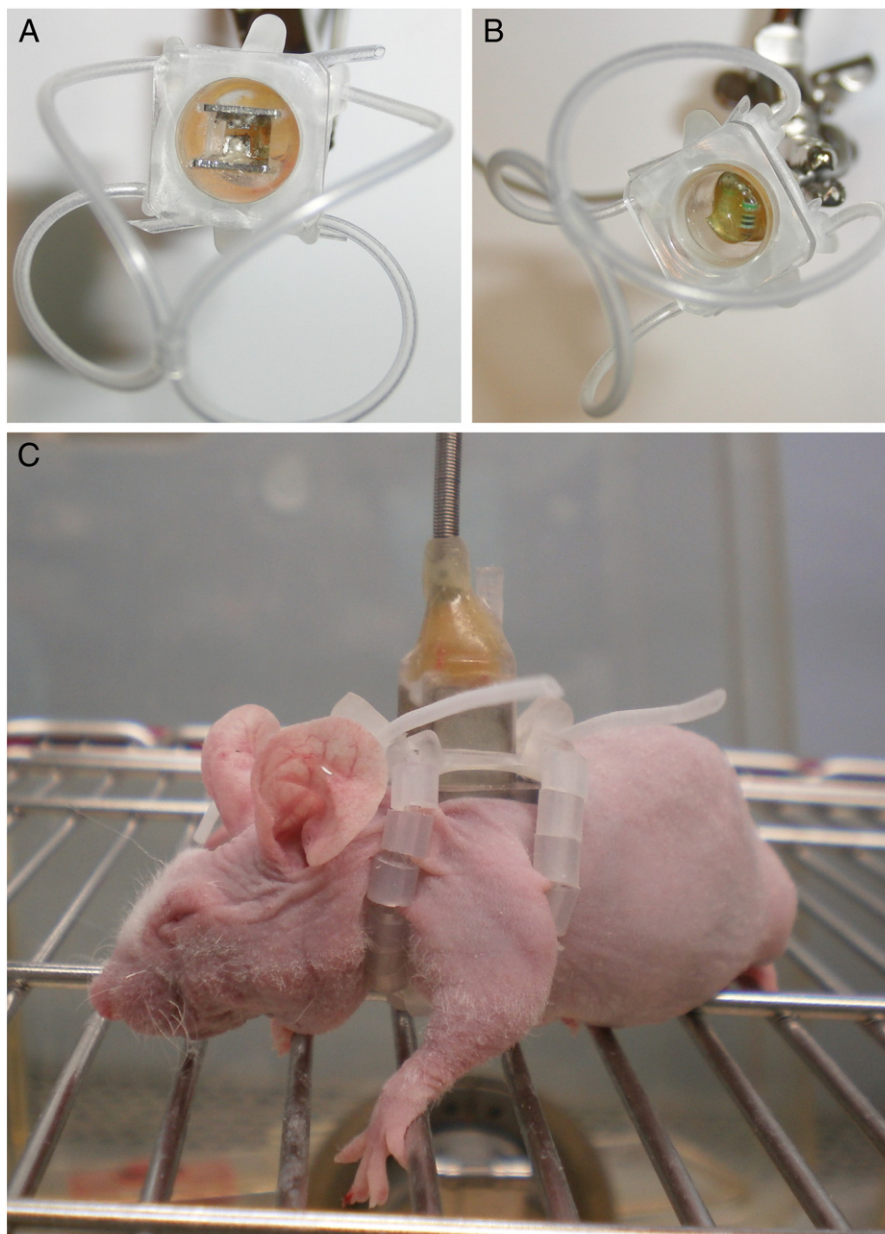
Fig. 1. Delivery system used during experiments. (A) Capsule to apply electric field treatments. (B) Capsule to apply hyperthermia treatments. (C) Mouse wearing a treatment capsule (animal lying on the top grid of the cage just before it is introduced into the cage and treatment begins).

on the difference between temperatures of the tissue and the arterial blood (T_b):

$$\rho c \frac{\partial T}{\partial t} = \nabla \cdot (k\nabla T) - \rho_b \omega_b c_b (T - T_b) + Q_m + Q. \quad (1)$$

The *Pennes Bioheat Equation* also takes into account the heat produced by the tissue metabolism (Q_m). In the present study this parameter was assumed as homogeneous in all the tissues ($Q_m = 420$ W/m^3) [18,22]. The same equation, under the assumption of no metabolic heat ($Q_m = 0$) and no blood perfusion ($\omega_b = 0$) was employed for obtaining the temperature within the inert materials of the capsule (e.g. PMMA and epoxy).

For thermal capsule simulations, heat delivery was modeled as a uniform source of power (P_r) over the volume (V_r) of the heating resistor:

$$Q = \frac{P_r}{V_r}. \quad (2)$$

In the electrical capsules, applied heat is due to Joule heating which is produced within materials that conduct electricity. Joule heating depends on the local electric field magnitude (E) and on the electrical conductivity of the material (σ):

$$Q = \sigma |E|^2. \quad (3)$$

The electric field distribution resulting from applying a voltage difference between both electrode plates was obtained by solving the
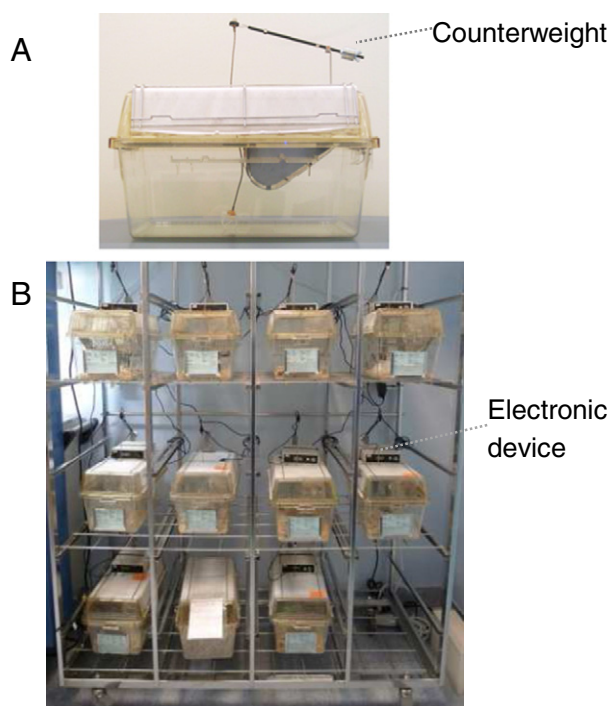
Fig. 2. (A) Animal cage with counterweight system supporting a treatment capsule. (B) Rack of cages with mounted treatment systems for parallel experiments.
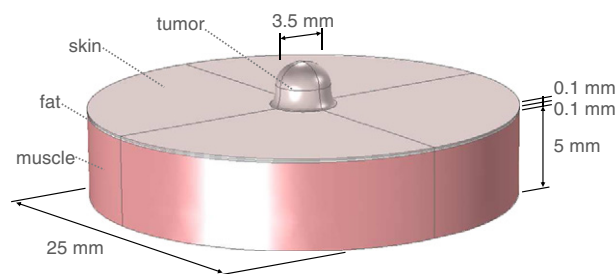

Scheme 3. Geometrical 3D model of mouse back section with a subcutaneous tumor.

The electrical and thermal material properties used in the model are summarized in Table 1. Those values were extracted from literature and from the FEM software library.

2.2. In vivo study

This study was approved and monitored by the IDIBELL Animal Care and Use Committee.

Five-week old male nude mice (Hsd: Athymic Nude-Foxn1nu) (Harlan Iberica, Spain) weighing 18–22 g were employed. The animals were housed in a sterile environment in cages with autoclaved bedding, food and water and were maintained on a daily 12-h light, 12-h dark cycle.

The study had three main consecutive stages: 1) subcutaneous tumor implantation at the back of the animal, 2) continuous treatment for a week with the wearable treatment capsules and 3) ex vivo tumor volume assessment.

The implanted tumor fragments were from xenograft TP11 from the pancreatic xenografts collection created in the Translational Research Laboratory in the ICO-IDIBELL [33]. Perpetuation of human tumors in athymic mice was performed in the following way: fresh 2 mm³ macroscopically viable fragments were orthotopically implanted in the body–tail of the pancreas. After implantation, tumor formation was checked weekly by palpation. When the tumor diameter was 1 cm approximately successive passages were performed in two animals until the fifth passage, when the tumor was considered perpetuated.

Tumor implantation for each batch of animals analyzed in this study was carried out in a single session. The surgical process for tumor implantation was carried out under anesthetic isoflurane inhalation. In this procedure, a fragment of about 25 mg of perpetuated exocrine human pancreatic adenocarcinoma was implanted subcutaneously in the interscapular area of the animal. In each session, all animals received tumor fragments from the same donor.

During the next week after implantation, the tumor was allowed to adhere and grow. After that week, daily measurements of external tumor size were performed with a digital caliper until a width of 3.5 mm was reached or surpassed. Then, the animal was randomly assigned to one of the four possible treatment groups (or to the respective control group) and treatment begun. Typically more than a single

electric potential (φ) that satisfies the Laplace equation (Eq. (4)).

$$\nabla \cdot (\sigma \nabla \varphi) = 0 \qquad (4)$$

To model heat flux towards ambient, an extra equation (Eq. (5)) was added at the external boundaries of the model. According to that equation, the total amount of thermal flux from a surface with unitary normal vector (n) depends on the heat transfer coefficient (h) and the temperature differences between constant ambient (T_{amb}) and surface (T). Values of 4 W/(m² K) [23] for heat transfer coefficient and ambient temperature of 22 °C were used.

$$-n \cdot (-k\nabla T) = h(T_{amb} - T) \qquad (5)$$

The simulated model represents a capsule (according to the geometries and materials represented in Figs. 1 and 2) on a subcutaneous tumor. The biological part of the model is composed of four different tissues: skin, tumor, fat and muscle. Its geometry is showed in Scheme 3 and it represents a cylindrical slab of the mice back with an embedded round shape for the subcutaneous tumor. A constant temperature of 37 °C was defined at the bottom side of the muscle tissue.

Table 1
Employed values of density (ρ), thermal conductivity (k), heat capacity (c), blood perfusion (w_b), electrical conductivity at 150 kHz (σ), relative permittivity at 150 kHz (ε_r) and the reference of these values. The non-referenced values were extracted from the COMSOL Multiphysics 4.3 library.

Material	ρ (kg/m³)	k (W/(m·K))	c (J/(kg·K))	w_b (kg/(m³·s))	σ (S/m)	ε_r ()	Reference
Skin	1010	0.42	3500	2.333	0.094	11362	[24,25]
Muscle	1040	0.50	3600	0.692	0.373	7109	[24,25]
Tumor	1000	0.64	3500	0.833	0.234	6850	[26,27]
Fat	920	0.25	2500	0.133	0.025	68	[24,25]
Blood	1060	–	3900	–	–	–	[24]
Gel	1000	0.60	4180	–	0.2	80	[15,28]
PMMA	1190	0.193	1420	–	1×10^{-15}	3	[29,30]
Electrodes	8000	15	480	–	7.4×10^6	1	[31]
Epoxy	1070	0.87	1419	–	–	–	[32]
Graphite	1950	150	710	–	–	–	–
Air	1.05	0.027	1006	–	–	–	–

Table 2
Treatment groups defined for the experiments. Control dose means the same setup but with a powerless electronic device.

Treatment group	Dose	Chemotherapeutic dose	n
Hyperthermia	41 °C		12
Hyperthermia control	Control		10
Hyperthermia + gemcitabine	41 °C	100 mg/kg (days 0, 3, 6)	8
Hyperthermia control + gemcitabine	Control	100 mg/kg (days 0, 3, 6)	8
TTFields	6 V/cm at 150 kHz		7
TTFields control	Control		6
TTFields + gemcitabine	6 V/cm at 150 kHz	100 mg/kg (days 0, 3, 6)	10
TTFields control + gemcitabine	Control	100 mg/kg (days 0, 3, 6)	7

animal reached the target tumor size at the same day. If two animals achieved this condition, one of them was assigned to the treatment (randomly chosen) and the other mouse was assigned to the respective control group. If a third animal also reached the size criterion for treatment initiation, then it was randomly assigned either to the treatment or to the control group already randomly chosen. If four animals simultaneously reached the size criterion for treatment, then the animals were paired according to their similarity in tumor size and randomly assigned to a treatment (and to the respective control group).

Table 2 summarizes the eight defined treatment groups and the dosage.

After one week of treatment the animal was sacrificed and the tumor mass was extracted to evaluate its final volume. Tissue samples were also collected for histological analysis.

Tumor volume (V) was estimated using Eq. (6) [34] from tumor width (W) and length (L) measurements performed with a digital caliper. The tumor growth ratio is defined by Eq. (7) where V_f is the final tumor volume and V_i is the volume when treatment began.

$$V = \frac{\pi}{6} \cdot L \cdot W^2 \qquad (6)$$

$$G = \frac{V_f - V_i}{V_i} \cdot 100 \qquad (7)$$

2.2.1. Chemotherapeutic drug

Gemcitabine was provided by the pharmacological department at the hospital. It was dissolved in buffered saline solution in a final concentration of 10 mg/ml. The administration schedule was on days 0, 3, and 6 after the treatment began and a dose of 100 mg/kg was administered by intraperitoneal injection. In previous studies we showed that the administration on days 0, 3, 6 and 9 was effective in inhibiting tumor growth [33,35]. We adapted this protocol in order to make it feasible for TTFields administration and to be able to evidence minor effects of TTFields on tumor growth reduction.

2.2.2. Histology and immunohistochemistry

At sacrifice, tumor samples were embedded in paraffin. With 3 μm slices, a hematoxylin–eosin staining and the immunostaining of Ki-67 using the monoclonal anti-Human Ki67, clone MIB-1 (Dako, Glostrup, Denmark) as a primary antibody and the anti-mouse EnVision System
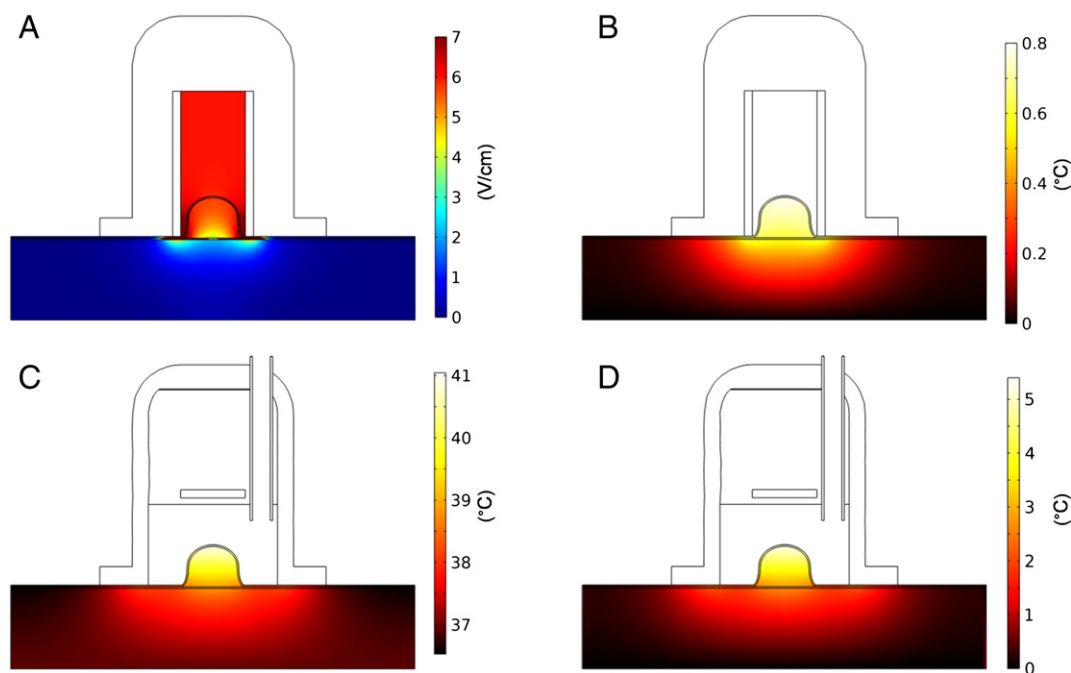

Fig. 3. Simulation results once thermal steady state has been reached (t = 30 min) (A) Electric field distribution when 2.4 V is applied across the electrode plates of the capsule for TTFields delivery. (Color range limited at 7 V/cm). (B) Increase of tissue temperature due to the applied electric field. (C) Tissue temperature distribution when a power of 99 mW is delivered through the heating resistor in the thermal capsule. (D) Increase of tissue temperature due to applied heating in the thermal capsule.
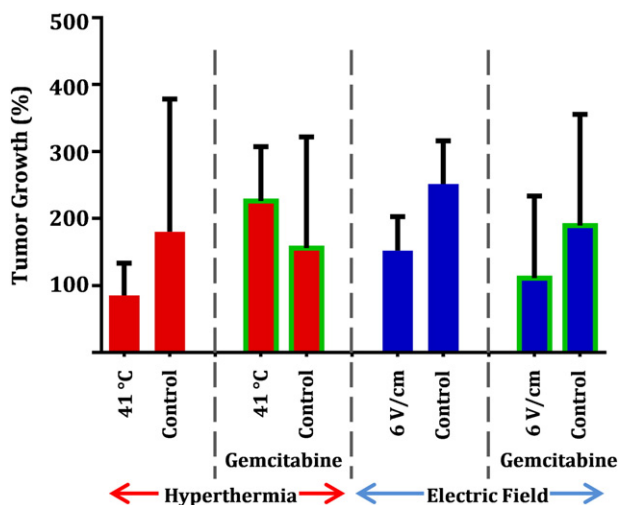
Fig. 4. Tumor growth for each treatment group. Data shown as median + interquartile range.

(Dako, Carpinteria, CA, USA) were performed. Tumor Ki67 + proliferation index was determined by counting the number of Ki67 + cellular nuclei relative to the total number of tumor cells.

2.2.3. Statistical analysis

Statistical analyses were performed with a specialized software package (SPSS v.19, IBM Inc., Chicago, IL, USA). Differences in tumor volume were compared by the two-tailed Mann–Whitney U test and also compared by the Wilcoxon matched-pairs signed rank test using matching pairs. Values of $p < 0.05$ were considered statistically significant in all comparisons.

2.3. Gel analysis

A quantitative analysis of metal ions in the conductive gel was carried out to discard any possible effect of electrochemically released ions from the electrodes on tumor growth. In particular, the concentration of metallic ions in gel samples that were kept in sealed electrical capsules subjected to the treatment (6 V/cm, 150 kHz) for a week was compared to equivalent samples from electrical capsules in which no electrical treatment was applied. The samples were analyzed for chromium (Cr), manganese (Mn), iron (Fe) and nickel (Ni) using inductively coupled plasma mass spectrometry (ICP-MS) by an external laboratory (CCiTUB, Barcelona, Spain).

3. Results

3.1. Treatment simulation

Simulation results for the electric field capsule indicate that delivery of a sinusoidal voltage wave at 150 kHz and 2.4 V of amplitude across the electrode plates produces a quite uniform field of about 6 V/cm in the space in between the electrode plates where the tumor is located (Fig. 3A). Temperature increase within tissues due to the electric field shows an average increment around 0.7 °C in the tumor with respect to the temperature when no field is applied (Fig. 3B).

Simulation results for the thermal capsule indicate that mean power of 99 mW is required to induce 41 °C on the top of the skin at the tumor location. Deeper into tissues the temperature decreases gradually (Fig. 3C). Tissue temperature increases up to 5 °C when hyperthermia treatment is applied (Fig. 3D).

Skin temperature measurements taken with a thermocouple during in vivo treatments confirmed that skin temperature increase for the electric field capsule was below 1 °C whereas skin temperature increase for the thermal capsule was about 4 to 5 °C.
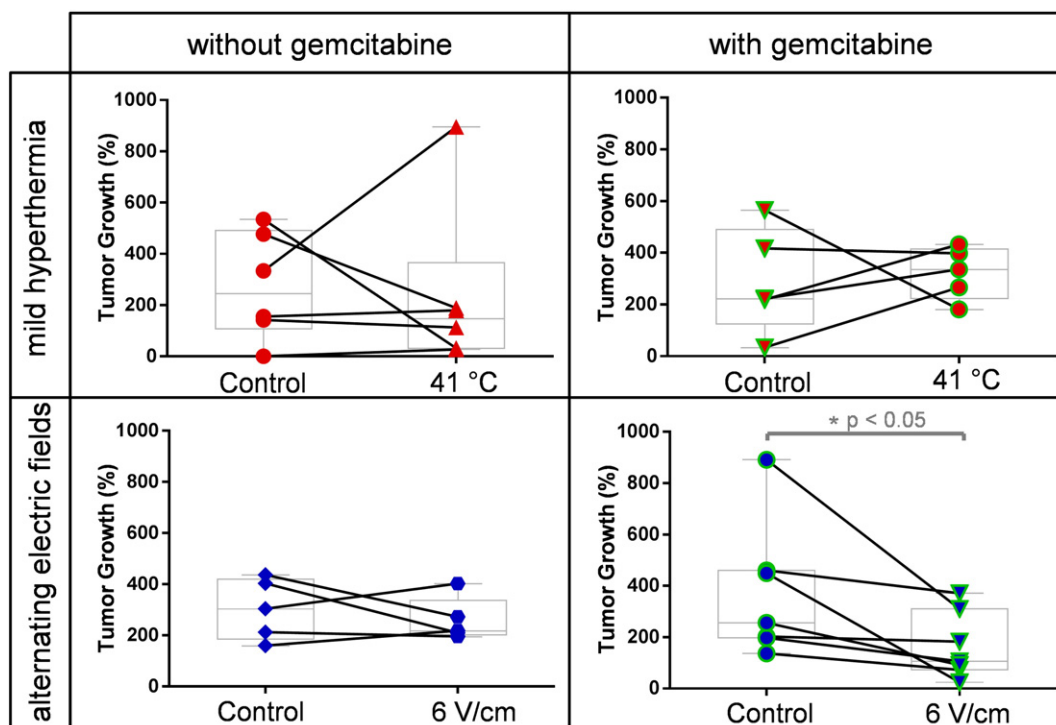

Fig. 5. Tumor growth results after a week using a paired analysis. Boxplots for each group and individual pairs are represented. (top left) Mild hyperthermia treatment. (top right) Mild hyperthermia as adjuvant. (bottom left) Alternating electric fields treatment. (bottom right) Alternating electric fields as adjuvant.

Table 3
Metallic ion concentrations in μg/g of conductive gel samples.

	Cr	Mn	Fe	Ni
One week in electrode capsule under AC field delivery (6 V/cm)	0.152	0.040	1.815	0.209
One week in electrode capsule (no electric field)	0.163	0.036	1.468	0.312
Non treated gel (out of the bag)	0.132	0.011	0.511	0.083

3.2. Treatment results

The administration of gemcitabine at the selected schedule in this patient-derived xenograft (PDX) did not inhibit tumor growth. Also, no significant differences in tumor growth became apparent when comparing hyperthermia and electric fields alone or in combination with gemcitabine (Mann–Whitney U test). However, we could not rule out a potential effect of the administered therapies due to the internal variability of each group that might be precluding the identification of significant differences among groups. Of note, this occurred in spite of having analyzed a good number of mice per group (Fig. 4).

During the preliminary trials exploring the in vivo setup (data not reported in here), it was observed that tumor fragments implanted in mice grew non-uniformly. Some of the fragments adhered easily and started growing fast and, in these cases, the minimum size required to start the treatment was achieved in few days. On the other hand, other tumor fragments remained small during longer periods and slowly grew up to the size required to start the treatment. These differences in tumor growth rate most likely persist once treatment begins and this surely has an impact on the results. Actually, it is highly plausible that this dispersion of initial tumor growth rates explains why no statistically significant differences are found between controls and treatments when the comparisons are performed at group level (Fig. 4).

Taking the above observation into account, and since a minor impact of any of the treatments on tumor growth was anticipated, the animals were artificially paired before treatment as it is described in Section 2.2 according to initial conditions (batch, tumor origin and initial tumor growth rate) so that a paired statistical analysis was also possible for tumor growth (Fig. 5). Not all the animals could be paired (14 of 68 animals) and these were disregarded in the paired analysis. On the other hand, on some occasions, rather than a single treatment animal and a single control animal, two treatment animals or two control animals were present. In these cases, the sample used for the paired analysis consisted in the average tumor size from the two considered animals. (It has been verified that by randomly selecting one or the other animal, instead of performing the average, the same qualitative results are obtained in terms of statistically significant differences between groups.)

In the paired analysis, mild hyperthermia did not show an effect on the tumor growth rate when six paired treated/non-treated pairs were compared (n = 6 + 6). Similarly, its combination with gemcitabine did not produce a significant effect when compared to the tumors only treated with chemotherapy (n = 5 + 5). Neither the alternating electric fields applied alone had any significant impact on tumor growth (n = 5 + 5). Nevertheless, each animal treated with the combination of electric field delivery and the administration of gemcitabine showed a lower tumor growth rate when comparing with their corresponding pairs treated alone with the drug (n = 7 + 7). Median tumor volume reduction in this group was 47%.

3.2.1. Histology and immunohistochemistry

The hematoxylin–eosin preparations displayed the expected histological features of the used tumor in all groups with some central necrotic parts without significant differences between groups. Statistical analysis of Ki67+ proliferation index between treatment groups and their respective control groups did not show statistical differences (Mann–Whitney U test).

3.3. Electrochemical release of metallic ions to the conductive gel

Table 3 summarizes the chromium (Cr), manganese (Mn), iron (Fe) and nickel (Ni) concentrations measured in treated and non-treated conductive gels.

4. Discussion

The results obtained here indicate that the proposed prolonged mild hyperthermia treatment does not have an impact on tumor growth rate, either applied singly or in combination with a chemotherapeutic drug. On the other hand, TTFields delivery had a positive impact on tumor growth when combined with the chemotherapeutic drug inducing a median reduction of tumor growth about 47%. A similar result has been reported in a previous in vivo study where TTFields combined with chemotherapy reduced by 52% the tumor growth when compared to chemotherapy alone [4].

It must be noted that, in the same experimental setup, TTFields delivery – despite producing less heating than the tried hyperthermia, as shown both by simulations and skin temperature measurements – had a positive impact on tumor growth whereas hyperthermia did not. Therefore, contrary to our hypothesis the modest beneficial impact of TTFields delivery on pancreatic tumor growth appears non-related with the induced temperature increase.

Both hyperthermia and TTFields offer better effectiveness when increasing the applied magnitude [1,13]. Therefore we decided to use the maximum magnitude that has been reported by TTFields promoters (6 V/cm) [5]. For hyperthermia treatments we used the maximum temperature that avoided any sort of damage to the mice skin (41 °C) as tested during the model set-up. In contrast to previously reported studies on the use of TTFields, we were not able to appreciate an impact of TTFields on tumor growth when applied singly, despite having doubled the field magnitude (6 V/cm) considered as maximum in previous clinical studies (3 V/cm). It must be noted that a preliminary batch of experiments (not reported here) showed no impact on tumor growth when delivering effective magnitudes of electric field of 1 V/cm to 3 V/cm [2], in line with a recent in vitro study [3].

One of the strengths of this study is its thorough and meticulous planning. In contrast to previous in vivo TTFields studies, here the animals were free to move within their cages. This made the design and the implementation of the treatment systems particularly challenging because robust systems were mandatory to reliably deliver the treatments during a whole week.

In previous studies TTFields had been applied using electrically insulated electrodes. These electrodes are covered by a thin dielectric layer of a high permittivity material so that DC currents are blocked whereas AC displacement currents can be injected. This prevents any possible electrochemical reactions at the electrodes that could produce species with some sort of physiological impact. However, a disadvantage of this strategy is that an uncertain portion of voltage drops at the dielectric layer rather than across the tissues which implies that the applied electric field is uncertain. In our case, in order to avoid such uncertainty, we used stainless steel electrodes in direct contact with the electrolytic gel and the tissues. Therefore, although DC currents were blocked in our electronic units (by a DC blocking capacitor), we wondered whether some electrochemically generated species could be responsible for the positive impact observed in the combination of TTFields delivery and chemotherapy and we decided to perform the analysis of the gel as reported in Sections 2.3 and 3.3. In principle, there was not much reason for concern because the applied frequency (150 kHz) would require much higher currents to produce a significant metallic release from electrodes [36]. And the metallic content analysis confirmed that: the analysis shows similar values in both treated

and control samples. Most likely the higher metallic content of both capsule samples in contrast to the brand new gel is due to diffusion. Therefore we can conclude that the observed tumor growth rate reduction is not related with electrochemically generated species during treatment.

We can only speculate about the mechanism of action for TTFields once it has become apparent that the induced mild hyperthermia is unrelated to the observed effect.

On the one hand, the obtained results show a slight synergy between the applied alternating electric field and the chemotherapeutic agent. On the other hand, tumor growth delay was not observed when the electric field is applied singly. Therefore, contrary to what has been reported by TTFields promoters, it seems that TTFields do not have a direct impact on tumor growth. Our observation is compatible with a scenario in which the delivery of alternating electric fields produces an increase of chemotherapeutic agent penetration. Previously increased endocytosis was observed when TTFields were observed at a higher frequency (900 MHz) but at the same range of magnitudes [37]. Endocytosis enhancement can be putatively linked to a better chemotherapeutic agent penetration [38].

The present study shows that concomitant chemotherapy and TTFields delivery have a beneficial impact on pancreatic tumor growth in a pre-clinical model consisting of pancreatic ductal adenocarcinoma perpetuated in athymic mice. Pancreatic ductal adenocarcinoma (PDAC) is one of the most aggressive solid tumors; and only 10 or 15% of patients are diagnosed when tumors are surgically resectable [39]. Poor response or resistance to current treatment modalities contributes to a poor prognosis for patients with advanced disease. At this stage, concomitant chemotherapy and TTFields delivery are encouraging for a tumor with such a dismal prognosis.

In the meanwhile further in vitro and in vivo studies are essential to confirm and validate this modest expectation. Should the delay in tumor growth be observed in other cancer model systems and an increment of the chemotherapeutic agent penetration be confirmed, the foundation for innovative therapeutic strategy could be laid. The application of fields for hours or days by means of portable systems is feasible through external electrodes over the body regions where the tumors were located. No surgical procedure would be required for directly applying the fields to the tumors through electrodes since the field magnitude of TTFields is low enough so as to be considered innocuous for the healthy tissues they would need to cross before reaching the tumors.

Acknowledgments

Appendix A. Supplementary data

Supplementary data to this article can be found online at http://dx.doi.org/10.1016/j.bioelechem.2015.04.006.

References

[1] E.D. Kirson, Z. Gurvich, R. Schneiderman, E. Dekel, A. Itzhaki, Y. Wasserman, et al., Disruption of cancer cell replication by alternating electric fields disruption of cancer cell replication by alternating electric fields, Cancer Res. 64 (2004) 3288–3295.
[2] A.M. Davies, U. Weinberg, Y. Palti, Tumor treating fields: a new frontier in cancer therapy, Ann. N. Y. Acad. Sci. 1291 (2013) 86–95, http://dx.doi.org/10.1111/nyas.12112.
[3] J. Liang, A.W. Mok, Y. Zhu, J. Shi, Resonance versus linear responses to alternating electric fields induce mechanistically distinct mammalian cell death, Bioelectrochemistry 94 (2013) 61–68, http://dx.doi.org/10.1016/j.bioelechem.2013.06.001.
[4] E.D. Kirson, R.S. Schneiderman, V. Dbalý, F. Tovarys, J. Vymazal, A. Itzhaki, et al., Chemotherapeutic treatment efficacy and sensitivity are increased by adjuvant alternating electric fields (TTFields), BMC Med. Phys. 9 (2009) 1, http://dx.doi.org/10.1186/1756-6649-9-1.
[5] E.D. Kirson, V. Dbalý, F. Tovarys, J. Vymazal, J.F. Soustiel, A. Itzhaki, et al., Alternating electric fields arrest cell proliferation in animal tumor models and human brain tumors, Proc. Natl. Acad. Sci. U. S. A. 104 (2007) 10152–10157, http://dx.doi.org/10.1073/pnas.0702916104.
[6] E.D. Kirson, M. Giladi, Z. Gurvich, A. Itzhaki, D. Mordechovich, R.S. Schneiderman, et al., Alternating electric fields (TTFields) inhibit metastatic spread of solid tumors to the lungs, Clin. Exp. Metastasis 26 (2009) 633–640, http://dx.doi.org/10.1007/s10585-009-9262-y.
[7] R.S. Schneiderman, E. Shmueli, E.D. Kirson, Y. Palti, TTFields alone and in combination with chemotherapeutic agents effectively reduce the viability of MDR cell sub-lines that over-express ABC transporters, BMC Cancer 10 (2010) 229, http://dx.doi.org/10.1186/1471-2407-10-229.
[8] R. Stupp, E.T. Wong, A. a Kanner, D. Steinberg, H. Engelhard, V. Heidecke, et al., NovoTTF-100A versus physician's choice chemotherapy in recurrent glioblastoma: a randomised phase III trial of a novel treatment modality, Eur. J. Cancer 48 (2012) 2192–2202, http://dx.doi.org/10.1016/j.ejca.2012.04.011.
[9] A. Chakravarti, Quantitatively determined survivin expression levels are of prognostic value in human gliomas, J. Clin. Oncol. 20 (2002) 1063–1068, http://dx.doi.org/10.1200/JCO.20.4.1063.
[10] R. Stupp, M.E. Hegi, M.R. Gilbert, A. Chakravarti, Chemoradiotherapy in malignant glioma: standard of care and future directions, J. Clin. Oncol. 25 (2007) 4127–4136, http://dx.doi.org/10.1200/JCO.2007.11.8554.
[11] J. Overgaard, D. Gonzalez Gonzalez, M.C.C.H. Hulshof, G. Arcangeli, O. Dahl, O. Mella, et al., Hyperthermia as an adjuvant to radiation therapy of recurrent or metastatic malignant melanoma. A multicentre randomized trial by the European Society for Hyperthermic Oncology, Int. J. Hyperth. 25 (2009) 323–334, http://dx.doi.org/10.1080/02656730903091986.
[12] X.-J. Yang, C.-Q. Huang, T. Suo, L.-J. Mei, G.-L. Yang, F.-L. Cheng, et al., Cytoreductive surgery and hyperthermic intraperitoneal chemotherapy improves survival of patients with peritoneal carcinomatosis from gastric cancer: final results of a phase III randomized clinical trial, Ann. Surg. Oncol. 18 (2011) 1575–1581, http://dx.doi.org/10.1245/s10434-011-1631-5.
[13] J. van der Zee, Heating the patient: a promising approach? Ann. Oncol. 13 (2002) 1173–1184, http://dx.doi.org/10.1093/annonc/mdf280.
[14] E.P. Armour, D. McEachern, Z. Wang, P.M. Corry, A. Martinez, Sensitivity of human cells to mild hyperthermia, Cancer Res. 53 (1993) 2740–2744.
[15] A. Ivorra, B. Al-Sakere, B. Rubinsky, L.M. Mir, Use of conductive gels for electric field homogenization increases the antitumor efficacy of electroporation therapies, Phys. Med. Biol. 53 (2008) 6605–6618, http://dx.doi.org/10.1088/0031-9155/53/22/020.
[16] A. Ivorra, B. Rubinsky, Electric field modulation in tissue electroporation with electrolytic and non-electrolytic additives, Bioelectrochemistry 70 (2007) 551–560, http://dx.doi.org/10.1016/j.bioelechem.2007.02.001.
[17] J.F. Edd, L. Horowitz, R.V. Davalos, L.M. Mir, B. Rubinsky, In vivo results of a new focal tissue ablation technique: irreversible electroporation, IEEE Trans. Biomed. Eng. 53 (2006) 1409–1415, http://dx.doi.org/10.1109/TBME.2006.873745.
[18] I. Lacković, R. Magjarević, D. Miklavčič, Three-dimensional finite-element analysis of joule heating in electrochemotherapy and in vivo gene electrotransfer, IEEE Trans. Dielectr. Electr. Insul. 16 (2009) 1338–1347, http://dx.doi.org/10.1109/TDEI.2009.5293947.
[19] N. Pavselj, Z. Bregar, D. Cukjati, D. Batiuskaite, L.M. Mir, D. Miklavčič, The course of tissue permeabilization studied on a mathematical model of a subcutaneous tumor in small animals, IEEE Trans. Biomed. Eng. 52 (2005) 1373–1381, http://dx.doi.org/10.1109/TBME.2005.851524.
[20] U. Pliquett, R. Nuccitelli, Measurement and simulation of Joule heating during treatment of B-16 melanoma tumors in mice with nanosecond pulsed electric fields, Bioelectrochemistry (2014) 1–7, http://dx.doi.org/10.1016/j.bioelechem.2014.03.001.
[21] H.H. Pennes, Analysis of tissue and arterial blood temperatures in the resting human forearm, J. Appl. Physiol. 85 (1998) 5–34.
[22] Y.-G. Lv, J. Liu, A theoretical way of distinguishing the thermal and non-thermal effects in biological tissues subject to EM radiation, Forsch. Ingenieurwes. 67 (2003) 242–253, http://dx.doi.org/10.1007/s10010-002-0098-8.
[23] D. a Nelson, S. a Nunneley, Brain temperature and limits on transcranial cooling in humans: quantitative modeling results, Eur. J. Appl. Physiol. Occup. Physiol. 78 (1998) 353–359.
[24] A. Ibrahiem, C. Dale, W. Tabbara, J. Wiart, Analysis of the temperature increase linked to the power induced by RF source, Prog. Electromagn. Res. 52 (2005) 23–46, http://dx.doi.org/10.2528/PIER04062501.
[25] S. Gabriel, R.W. Lau, C. Gabriel, The dielectric properties of biological tissues: II. Measurements in the frequency range 10 Hz to 20 GHz. Phys. Med. Biol. 41 (1996) 2251–2269.
[26] J. Lang, B. Erdmann, M. Seebass, Impact of nonlinear heat transfer on temperature control in regional hyperthermia, IEEE Trans. Biomed. Eng. 46 (1999) 1129–1138.
[27] S. Laufer, A. Ivorra, V.E. Reuter, B. Rubinsky, S.B. Solomon, Electrical impedance characterization of normal and cancerous human hepatic tissue, Physiol. Meas. 31 (2010) 995–1009, http://dx.doi.org/10.1088/0967-3334/31/7/009.

[28] S.M. Becker, a V. Kuznetsov, Local temperature rises influence in vivo electroporation pore development: a numerical stratum corneum lipid phase transition model, J. Biomech. Eng. 129 (2007) 712–721, http://dx.doi.org/10.1115/1.2768380.

[29] M. Gad-el-Hak, W. Seemann, MEMS handbook, Appl. Mech. Rev. 55 (2002) B109, http://dx.doi.org/10.1115/1.1508147.

[30] J. Brandup, E. Immergut, E. Grulke, Polymer Handbook, John Wiley & Sons, Inc., 1999

[31] E.J. Berjano, F. Burdío, A.C. Navarro, J.M. Burdío, A. Güemes, O. Aldana, et al., Improved perfusion system for bipolar radiofrequency ablation of liver: preliminary findings from a computer modeling study, Physiol. Meas. 27 (2006) N55–N66, http://dx.doi.org/10.1088/0967-3334/27/10/N03.

[32] A. Kholodenko, V. Riadovikov, H. Moser, The Thermal and Mechanical Properties of Glues for the Atlas SCT Module Assembly, 2000. (CERN-ATL-INDET. 007).

[33] M. Vives, M.M. Ginestà, K. Gracova, M. Graupera, O. Casanovas, G. Capellà, et al., Metronomic chemotherapy following the maximum tolerated dose is an effective antitumour therapy affecting angiogenesis, tumour dissemination and cancer stem cells, Int. J. Cancer 133 (2013) 2464–2472, http://dx.doi.org/10.1002/ijc.28259.

[34] M.M. Tomayko, C.P. Reynolds, Determination of subcutaneous tumor size in athymic (nude) mice, Cancer Chemother. Pharmacol. 24 (1989) 148–154, http://dx.doi.org/10.1007/BF00300234.

[35] B. Laquente, C. Lacasa, M.M. Ginestà, O. Casanovas, A. Figueras, M. Galán, et al., Antiangiogenic effect of gemcitabine following metronomic administration in a pancreas cancer model, Mol. Cancer Ther. 7 (2008) 638–647, http://dx.doi.org/10.1158/1535-7163.MCT-07-2122.

[36] J. Morren, B. Roodenburg, S.W.H. de Haan, Electrochemical reactions and electrode corrosion in pulsed electric field (PEF) treatment chambers, Innov. Food Sci. Emerg. Technol. 4 (2003) 285–295, http://dx.doi.org/10.1016/S1466-8564(03)00041-9.

[37] N. Mahrour, R. Pologea-Moraru, M.G. Moisescu, S. Orlowski, P. Levêque, L.M. Mir, In vitro increase of the fluid-phase endocytosis induced by pulsed radiofrequency electromagnetic fields: importance of the electric field component, Biochim. Biophys. Acta 1668 (2005) 126–137, http://dx.doi.org/10.1016/j.bbamem.2004.11.015.

[38] L.M. Bareford, P.W. Swaan, Endocytic mechanisms for targeted drug delivery, Adv. Drug Deliv. Rev. 59 (2007) 748–758, http://dx.doi.org/10.1016/j.addr.2007.06.008.

[39] J. Busquets, J. Fabregat, R. Jorba, F.G. Borobia, C. Valls, T. Serrano, et al., Indications and results of pancreatic surgery preserving the duodenopancreatic region, Cir. Esp. 82 (2007) 105–111.